Single-Stroke Rotary Deep Hole Drilling of Stainless Steel Using Low-Pressure Nano-Fluid Lubrication

Van-Du Nguyen
Faculty of International Training, Thai Nguyen University of Technology, Thai Nguyen City, Vietnam
vandu@tnut.edu.vn

Thu-Ha Mai
Thai Nguyen High School for Gifted Students, Thai Nguyen City, Vietnam
maiha180184@gmail.com

Ky-Thanh Ho
Faculty of Mechanical Engineering, Thai Nguyen University of Technology, Thai Nguyen City, Vietnam
hkythanh@tnut.edu.vn (corresponding author)

Received: 24 July 2025 | Revised: 9 September 2025 | Accepted: 15 September 2025

 DOI: https://doi.org/10.48084/etasr.13620

ABSTRACT

This study demonstrates a novel, low-cost lubrication technique that enables single-stroke deep hole drilling of SUS 304 stainless steel using a rotary twist drill with internal coolant channels. A graphene-based nanofluid, formulated by dispersing graphene nanosheets into a water-soluble emulsion and diluted with tap water, was internally delivered at low pressure (1.5 bar) and low flow rate (0.25 L/min). Comparative trials under varying cutting conditions (spindle speeds: 430–870 rev/min and feed rates: 0.04–0.10 mm/rev) revealed that drilling with the proposed nanofluid produced chips with favorable morphology and manageable length, facilitating efficient evacuation. In contrast, conventional emulsion generated crushed chips prone to clogging. The graphene-based nanofluid also significantly reduced the thrust force and extended the tool life, enabling stable deep-hole drilling without pecking or tool failure. Statistical analysis and Taguchi optimization confirmed the robustness of the proposed approach. Unlike high-pressure or ultrasonic-assisted systems, the proposed method offers a simple and energy-efficient solution for machining hard-to-cut materials under realistic manufacturing conditions.

Keywords-nano-fluid; deep hole drilling; hard-to-cut materials; thrust force; tool wear

I. INTRODUCTION

Drilling is a primary machining process for producing circular holes and accounts for about 25% of the total machining time [1]. As the hole depth increases, particularly when the Length-to-Diameter (L/D) ratio exceeds five, commonly referred to as deep-hole drilling [2, 3], the process becomes significantly more difficult due to chip congestion, heat buildup, and restricted coolant flow. These issues lead to higher cutting forces, reduced tool life, and poor surface finish [4], particularly in stainless steels, which are known for their low thermal conductivity, strain hardening, and strong tool adhesion [5]. Precision requires optimizing tool geometry, coating, chip evacuation, and lubrication strategies. Solid carbide twist drills are preferred for their performance over single-lip drills [6, 7], though ensuring effective lubrication delivery remains a key challenge [8, 9]. Poor chip evacuation and coolant access can ultimately cause tool breakage and dimensional errors [10, 11].

To address these problems, various approaches have been explored. For example, peck drilling enhances chip evacuation and lubricant access by intermittently retracting the tool. Experiments on AISI 1045 and D2 steels under Minimum Quantity Lubrication (MQL) and flood lubrication showed improvements in tool life and hole geometry [2, 12]. However, peck drilling increases the machining time, requires CNC automation, and may cause chip fallback, degrading surface finish and accelerating wear [13]. MQL is an environmentally friendly approach that uses compressed air with minimal oil to reduce friction and heat. For deep holes (L/D > 15), elevated pressures (6–8 bar) and dual-channel nozzles are required [14]; however, the cooling performance remains limited, particularly with low thermal conductivity materials. Experimental trials on AISI 304 and 316 stainless steels revealed fewer completed

holes under MQL compared to 60-bar flood cooling [15]. Although internal MQL at 10 bar is proposed for steels, such as AISI 4144 M [16], its high system complexity and cost limit its broader adoption in conventional workshops. Ultrasonic-Assisted Drilling (UAD) applies high-frequency axial vibrations to enhance chip fragmentation and reduce cutting forces. Several studies have demonstrated improved deep-hole drilling performance of steel and SUS 304 stainless steel under different lubrication environments [17-19]. However, UAD faces critical limitations when drilling deep holes in stainless steel. The transducer and horn occupy the rear end of the tool, preventing internal lubrication, which is vital for managing heat and chip adhesion in low-conductivity materials. Additionally, UAD requires precise resonance tuning for each tool geometry, making it costly and inflexible for industrial applications. High-pressure internal cooling systems, typically operating at 40 bar or higher, enhance chip evacuation and thermal control during deep-hole drilling [16, 20]. Tests using internally lubricated twist drills on AISI 304 and 316 stainless steels showed improved chip breaking and surface finish [15]. However, their high energy demands, infrastructure costs, and fluid stability requirements present safety and maintenance challenges, limiting broader adoption. To reduce the reliance on high-pressure systems and improve energy efficiency, researchers have investigated nanofluid lubrication, which incorporates nanoparticles, such as graphene, MoS_2, SiO_2, and Al_2O_3, to enhance heat transfer, reduce friction, and improve wettability, leading to better chip evacuation and tool longevity [21-23]. However, nanofluids often use viscous cutting or vegetable oils that hinder internal delivery, and water-based variants require deionized water to maintain stability, increasing system complexity [24].

To address these constraints, the present work introduced a graphene-based nanofluid specifically designed for internal lubrication [17, 25]. This nanofluid was formulated by dispersing graphene nanosheets into a water-soluble emulsion and then diluting the mixture with ordinary tap water, achieving a stable, low-viscosity suspension that eliminated the need for costly deionized water, which is often required in conventional nanofluid formulations [24]. The approach enabled single-stroke deep drilling of SUS 304 stainless steel (L/D = 8) using a stationary twist drill under low-pressure (1.5 bar) and low-flow (0.25 L/min) conditions and without reliance on pecking, ultrasonic assistance, or high-pressure systems. While this method proved effective, the experimental setup used a stationary drill configuration, where the drill remained fixed while the workpiece rotated. This configuration is inherently less demanding in terms of heat generation, chip-tool-wall interaction, and tool wear. In contrast, rotary drilling, which is common in industrial machining, introduces higher thermal loads, more aggressive chip evacuation demands, and accelerated tool degradation, making effective lubrication significantly more challenging. Therefore, applying this water-based nanofluid under realistic rotary-drilling conditions remains unverified.

To address this gap, the current study investigates the same graphene-based nanofluid lubrication technique in a rotary deep-drilling setup, using a 5 mm twist drill with internal coolant holes to perform continuous through-hole drilling of SUS 304. A comparative analysis between the proposed nanofluid and conventional emulsion lubrication was conducted to evaluate the thrust force, chip morphology, and tool wear. The results demonstrate that the graphene nanofluid continues to offer significant advantages under rotary conditions, such as maintaining low cutting forces, stable performance, and extended tool life, thereby confirming its potential as a practical and cost-effective solution for the industrial machining of difficult-to-cut materials. In summary, this study presents three key findings: (1) A low-cost, internally delivered graphene-based nanofluid that performs effectively under low-pressure and low-flow conditions, in contrast to conventional high-pressure or ultrasonic-assisted lubrication systems. (2) A practical formulation that utilizes tap water instead of deionized water, enhancing scalability and shop-floor applicability. (3) An extension of nanofluid lubrication to rotary twist drilling, a more demanding process than stationary setups, demonstrating improved chip morphology, reduced thrust force, and extended tool life under real-world machining conditions.

II. MATERIALS AND METHODS

A. Experiment Setup

A 5-mm diameter twist drill bit from Nachi Inc. (model AQUA DEXOH8D) featuring two small internal coolant holes was utilized. The drill bit had a flute length of 55 mm and a point angle of 135°. The experiments were conducted using a conventional milling machine (model 2UMB, Niigata, Japan). Figure 1 illustrates the experimental setup, with the schematic presented in Figure 1(a) and the practically implemented system in Figure 1(b).

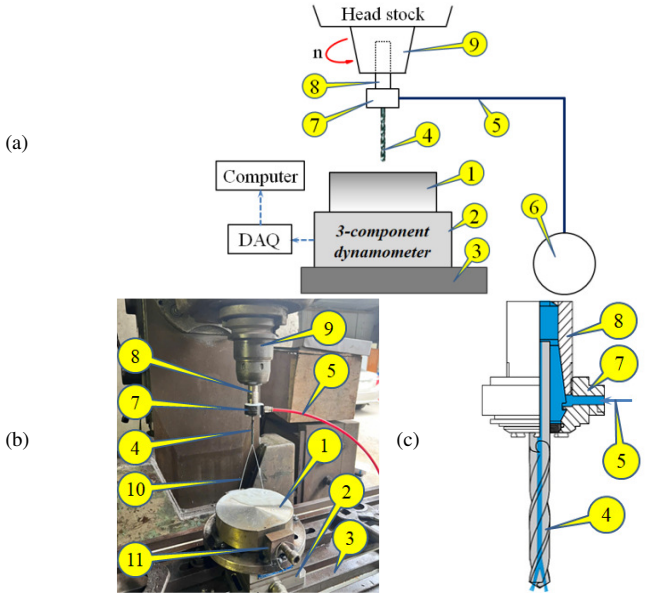

Fig. 1. The experimental setup: (a) schematic arrangement, (b) actual implementation captured in a photograph, and (c) operational principle of the reCool system.

As shown in Figure 1, the drill bit (4) is clamped inside a hollowed collet (8), which is secured within the spindle (9).

The hollowed collet (8) is enclosed by the set reCool system (7) made by RegoFix Inc., allowing a lubricant fluid to flow through the reCool system and the hollowed collet to supply the coolant directly into the drill bit. A small pump (6), using a commercial windshield washer pump for automobiles, delivers a 1.5 bar pressure and a 0.25 L/min flow rate through the two small coolant holes in the drill bit via a tube (5). The pump operates at 12 VDC, with a power consumption of 24 W. The workpiece (1) is fixed by a jig (11), which is clamped on the top surface of a Kistler 9257B (Kistler, USA) three-component force sensor (2), enabling thrust force measurement during drilling. As depicted in Figure 1(b), coolant fluid (10) is delivered through the drill bit's internal channels. Figure 1(c) portrays the principle of operation of the reCool system.

B. Preparing Materials and Lubricant Fluid

A commercially available SUS 304 stainless steel bar with a 150-mm diameter was selected and subsequently sliced by EDM wire-cut to a height of 40 mm for the experiments. During the experiment, the workpiece was continuously drilled through its height, i.e., with an aspect ratio length-to-diameter of 8 (L/D = 40/5).

The nanofluid used was a mixture of nano-emulsion and normal tap water, with a volumetric ratio of 10 vol. % nano-emulsion to 90 vol. % tap water. Graphene nanosheets and the Caltex Aquatex 3180 soluble oil were selected as raw materials for lubricant preparation. The former were synthesized using a plasma-induced method. Their morphology and structural characteristics were analyzed through Transmission Electron Microscopy (TEM) (JEM-2100F, JEOL, Japan). The graphene nanosheets had an average thickness of 2–10 nm and an average width of 1–4 μm (Figure 2(a)). Caltex Aquatex 3180 soluble oil was selected as the emulsifying fluid. When mixed with water, it forms a stable, milky-white emulsion and is widely used as a lubricant in various machining operations.

The lubricant was prepared following a two-step process, as described in [25]. The first step in preparing the lubricant was mixing the nanoparticles with the base medium. An ultrasonic horn cleaner was used to disperse the graphene into the emulsion fluid. During this stage, ultrasonication was performed at a frequency of 28 kHz for 30 min to ensure uniform distribution of the nanoparticles in the emulsion medium. The base fluid containing the nanoparticle-emulsion mixture was prepared at a concentration of approximately 0.1 wt%, corresponding to 100 mg of nanoparticles mixed with 100 mL of emulsion.

In the second step, the nano-emulsion was stirred with normal tap water. Since the emulsion is soluble in water, the final lubricant fluid could be easily prepared, provided that careful attention was given to the proportion of each component. A typical ratio of 10 vol% nano-emulsion and 90 vol% normal tap water, as proposed by manufacturers, was used in this study. To verify whether the nanosheets were fully dispersed in the base fluid, micrographs were taken 24 h after mixing using an Insize microscope at a scale of 100. A micrograph of the final nanofluid, consisting of 90 vol% water and 10 vol% nano-emulsion, is presented in Figure 2(b). In this image, the nanosheets appear as dark dots, indicating successful distribution without agglomeration, even after 24 h.

(a)

(b)

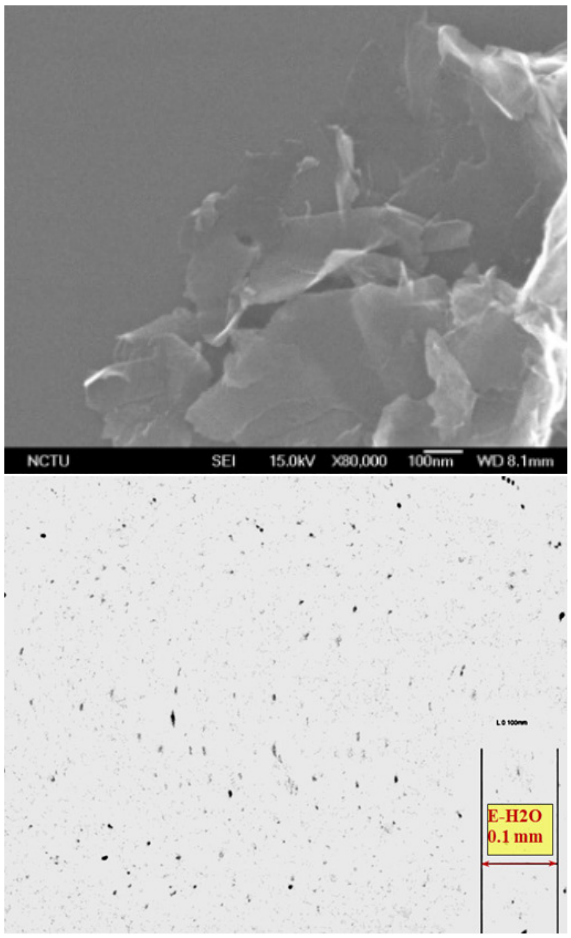

Fig. 2. (a) TEM image of graphene nanosheets and (b) nanofluid prepared from nano-emulsion and water, photographed after 24 h of mixing.

The conventional emulsion fluid was prepared by mixing the soluble oil Caltex Aquatex 3180 with fresh water at volumetric ratios of 10 vol% and 90 vol%, respectively.

C. Experiment Design

This study implemented four sets of experiments. First, pilot tests were conducted to compare two lubricant types: (i) a conventional emulsion fluid without nanosheets and (ii) a graphene-based nanofluid, using hole completion as the evaluation criterion for drilling capacity. Second, the effects of the lubricant on the thrust force and chip morphology were analyzed, and a two-sample t-test was used to assess the effect of both lubricant fluids on the thrust force. Third, a Taguchi design was applied to efficiently select the proper cutting parameters for nano-lubricant drilling. Finally, a validation test was conducted using the selected proper cutting parameters. The thrust force distribution and tool wear during drilling with two types of cooling lubricants were analyzed in detail in this experiment.

In each drilling test, the lubricant fluid was delivered into the drilling zone through the internal coolant holes of the drill bit under low-pressure and low-flow conditions, specifically at a pressure of 1.5 bar and a flow rate of 0.25 L/min. The effectiveness of the proposed nanofluid in improving the cutting performance was assessed by comparing the thrust force, chip morphology, number of completed holes, and tool wear with those of the conventional emulsion fluid. Although the drill bit is designed for drilling SUS 304 stainless steel with L/D > 5, the manufacturer proposes peck drilling with step feeds of 0.2D to 1.0D. However, all tests in this study were conducted under more demanding conditions. Through-holes with L/D = 8 were continuously drilled without pecking. Each test utilized a new drill bit, with cutting parameters selected based on the manufacturer's guidelines and the existing literature.

III. RESULTS AND DISSCUSION

A. Pilot Test

The main objective of the pilot test was to evaluate the ability to successfully complete deep hole drilling on the workpiece. To ensure consistency, a new drill bit was used for each test. The obtained results are presented in Table I.

As observed in Table I, the emulsion fluid without nanosheets successfully completed hole drilling only at a lower feed rate of 0.06 mm/rev for all spindle speeds. At a feed rate of 0.06 mm/rev, the hole was completed only at spindle speeds of 430 and 610 rpm. However, at a higher feed rate of 0.10 mm/rev, this lubricant fluid was unable to complete the drilling process, and the drill bits were braking. In contrast, drilling using the proposed nanofluid lubrication was successfully completed for all cutting parameters.

TABLE I. EXPERIMENT SETTINGS AND DRILLING ABILITY USING THE TWO LUBRICANTS

No	Cutting parameters		Types of lubricant fluid	
	Spindle speed (rev/min)	Feed rate (mm/rev)	Emulsion-fluid	Nanofluid
1	430	0.04	√	√
2	610	0.04	√	√
3	870	0.04	√	√
4	430	0.06	√	√
5	610	0.06	√	√
6	870	0.06	X	√
7	430	0.10	X	√
8	610	0.10	X	√
9	870	0.10	X	√

B. Effects of Lubrication Fluid on Thrust Force and Chip Morphology

Figure 3 illustrates the thrust forces obtained at a feed rate of 0.06 mm/rev using the two lubricant fluids in relation to the L/D ratio. The results indicate that the thrust forces during drilling with the graphene-based nanofluid (Figure 3(a)) remained stable across all feed rates and spindle speeds. In contrast, when the emulsion fluid without nanoparticles was used (Figure 3(b)), the thrust forces were initially stable but increased significantly toward the end of the drilling process. This phenomenon could be the result of chips jamming during the drilling process [4].

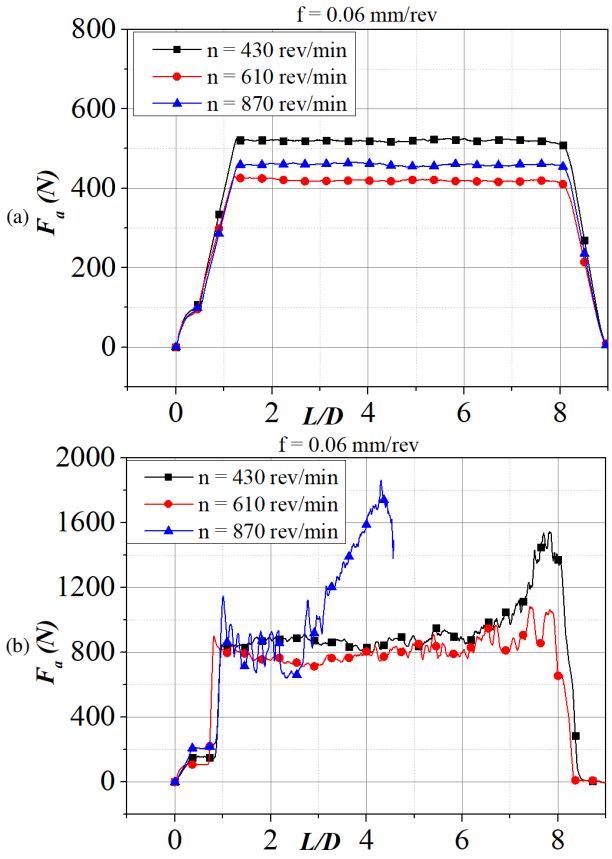

Fig. 3. Thrust forces obtained from drilling processes using: (a) the proposed nanofluid and (b) a typical emulsion fluid.

To further demonstrate the chip evacuation efficiency, Figure 4 presents examples of drilling using the two lubricants. Drilling with the graphene-based nanofluid produced short, separated string chips of relatively uniform length, as shown in Figure 4(b). Additionally, after drilling with the nanofluid, almost no chip adhesion was observed on the drill bit surface (Figure 4(a)). The relatively uniform and moderate chip length observed when using the graphene-based nanofluid contributed to smoother chip evacuation, reducing the likelihood of clogging and maintaining stable cutting conditions throughout the drilling process. Conversely, when the typical emulsion fluid was used, the chip lengths varied considerably, as displayed in Figure 4(d). In the early stages of the drilling process, the chips were relatively long, but then gradually became shorter and finely broken as the stroke depth increased. Consequently, when drilling with the conventional emulsion fluid without nanosheets, the chips adhered tightly to the drill flutes (Figure 4(c)), contributing to increased thrust forces.

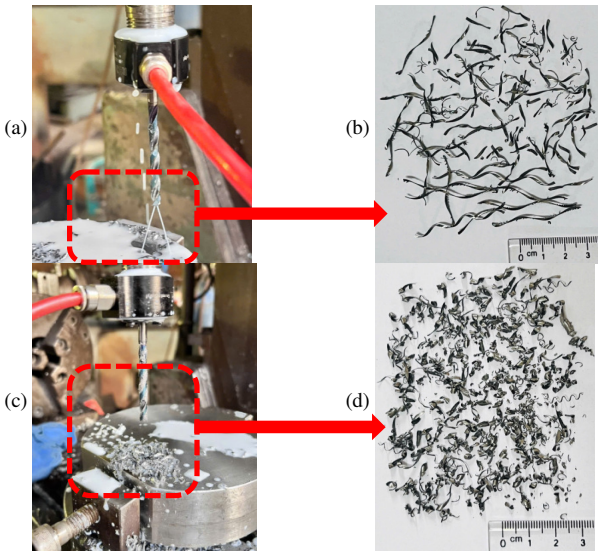

Fig. 4. Images of drill bits and chip morphology after drilling (a, b) with the proposed nanofluid and (c, d) with the conventional emulsion.

Figure 5 presents longitudinal sections of the drilled holes. In the case of an incomplete hole drilled using emulsion fluid (Figure 5(a)), broken chips clogged the drill flutes, hindering evacuation as the hole depth increased. This obstruction resulted in an elevated thrust force and ultimately led to drill-bit failure (blue line in Figure 3(b)). The completed hole drilled with the emulsion fluid, as depicted in Figure 5(b), exhibited a noticeable expansion in diameter near the final drilling depth. This expansion was likely caused by chip clogging, which complicated the evacuation, increased the thrust force (black line in Figure 3(b)), and contributed to localized enlargement at the chip-clogged site. Conversely, the hole drilled using the proposed nanofluid (Figure 5(c)) maintained a uniform diameter with a significantly smoother surface finish compared to the previous two cases.

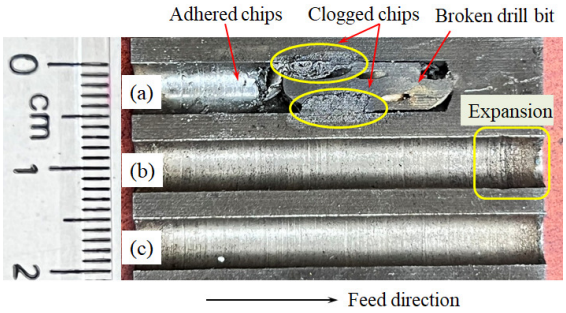

Fig. 5. Longitudinal sections of drilled holes: (a) incomplete using emulsion fluid, (b) completed using emulsion fluid, and (c) completed using nanofluid.

The morphology of the chips generated using the two lubricants is depicted in the images presented in Figures 6 and 7. These figures illustrate that the width of the chips formed during drilling with the proposed nanofluid was significantly narrower than that produced using the conventional emulsion fluid. As shown in Figure 6, the presence of waves on the back surface of the chips indicates bending during the evacuation process. The peaks of these waves, aligned against the flutes and hole wall, appear notably brighter, whereas the bases are darker. The wave frequency observed when drilling with the nanofluid was lower than that obtained with the emulsion fluid, suggesting a more controlled and efficient machining process. Additionally, the chips obtained when drilling with the nanofluid (Figure 6(a)) exhibited few distinctly spaced large cracks along their edges. In contrast, the chips generated with the emulsion fluid (Figure 6(b)) displayed a greater number of large cracks that were more closely clustered.

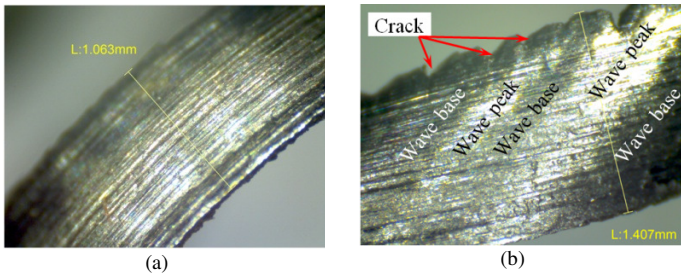

Fig. 6. Morphology of the back surface of the drilled chips (200× magnification) using: (a) the proposed nanofluid, and (b) a conventional emulsion-fluid.

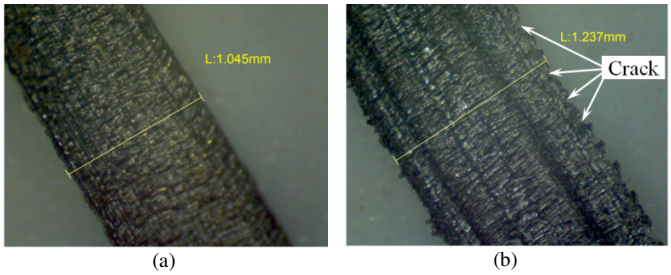

Fig. 7. Morphology of the free surface of the obtained chips (200× magnification) using: (a) the proposed nanofluid, and (b) a conventional emulsion-fluid.

These critical observations can be attributed to several factors. First, during the drilling process using nanofluids, the tribo-film effect forms between the chip surface and the hole wall, as well as between the chip surface and the flute surface [26]. Additionally, incorporating nanoparticles into the lubricant reduces the friction coefficient [21], further enhancing its lubricating effect. This improvement in lubrication minimizes sliding friction, leading to a reduction in thrust forces, as shown in Figures 3(a) and (b), and consequently resulting in less chip bending (Figure 6(a) compared to Figure 6(b)). Second, the heat dissipation effect of the lubricating fluid is enhanced when mixed with nanosheets [21, 26], which contributes to reducing the chip temperature and adhesion, thereby improving chip evacuation and minimizing the likelihood of tool clogging. Consequently, fewer large cracks were observed on the chip edges (Figures 6(a) and 7(a)), thereby mitigating chip crushing typically encountered at increased drilling depths with conventional emulsion-based lubrication (Figure 4(d)).

In contrast, deep-hole drilling under conventional emulsion lubrication resulted in intense chip shrinkage and significant contact friction during evacuation, leading to the formation of large cracks along the chip edges (Figures 6(b) and 7(b)). These cracks made the chips more prone to fine fragmentation as the drilling depth increased (Figure 4(c)). The increased chip deformation observed when using the emulsion fluid contributed to the increase in the thrust force. This correlation between chip morphology and cutting force has been documented in [27].

To evaluate the effectiveness of the graphene-based nanofluid compared to the emulsion fluid, a two-sample t-test was conducted to examine the statistical differences between the two lubricant populations. Based on the experimental datasets, the two-sample t-test yielded statistically significant results. For the comparison process, the maximum thrust force for each drilled hole under both lubricants, nanofluid and emulsion fluid, was selected as the key parameter. The results are presented in Figure 8, and the corresponding data are summarized in Table II.

TABLE II. RESULTS OF THE TWO-SAMPLE T-TEST

Factor	Lubricant fluid	Mean	Standard deviation	SE mean	Difference estimated	95% CI for difference	p-value
Thrust force, F_{amax}	Emulsion-fluid	1461	382	127	862	(563, 1162)	0.000
	Nanofluid	599	107	36			

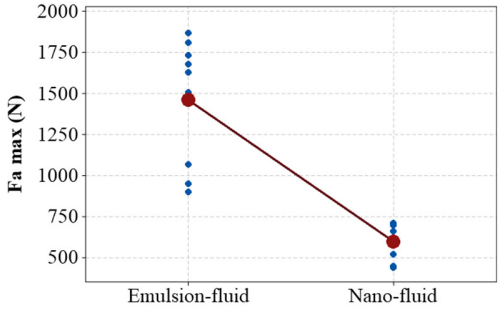

Fig. 8. Results of the two-sample t-test of the maximum thrust force.

Figure 8 illustrates that the mean values of the maximum thrust force when using the nanofluid are significantly lower than those with the emulsion fluid. Additionally, the results indicate that the thrust force exhibited considerably smaller fluctuations when using the nanofluid compared with the emulsion fluid. Table II further confirms that the mean values of the maximum thrust force with the nanofluid are consistently lower than those obtained with the emulsion fluid. Moreover, the standard deviations, which reflect the range of fluctuations for each factor, are notably smaller when using the graphene-based nanofluid, highlighting its stabilizing effect. The underlying mechanism of this remarkable phenomenon is likely attributed to the positive influence of the nanosheets, as documented in [21, 26].

With a p-value significantly smaller than 0.05, it can be confirmed that the thrust force when deep drilling under the graphene-based nanofluid is significantly lower than that observed with the conventional emulsion fluid. Additionally, statistical inference with 95% confidence intervals, none of which include zero, demonstrates that there are significant differences between the means of the two populations.

C. Selection of Cutting Parameters

To quickly select the proper cutting parameters when a graphene-based nanofluid is used as a lubricant, a Taguchi experimental design was conducted. Taguchi designs utilize orthogonal arrays, enabling the independent investigation of each factor's effect while minimizing the time and experimental costs. In this study, two control factors (spindle speed and feed rate), each with three levels, were selected, as shown in Table III. A standard Taguchi experimental plan L9 was employed to efficiently determine the optimal cutting parameters when using a graphene-based nanofluid as a lubricant. The response variable was defined as the maximum thrust force recorded in each test. Given that the objective was to minimize the thrust force, the smaller-is-better Signal-to-Noise (S/N) ratio was selected. The optimal factor levels correspond to those that yield the smallest mean. Additionally, in Taguchi experiments, it is proposed to maximize the S/N ratio to enhance robustness.

TABLE III. EXPERIMENTAL PARAMETERS AND THEIR LEVELS

Parameters	Levels		
	Low	Middle	High
Spindle speed *n* (rev/min)	430	610	870
Feed rate *f* (mm/rev)	0.04	0.06	0.10

The experimental results are presented in Table IV, whereas the main effects' plots for the maximum thrust force (F_{amax}) and S/N ratios are illustrated in Figure 9. As shown in Figure 9(a), the cutting parameter set with a spindle speed of 610 rev/min and feed rate of 0.06 mm/rev yielded the smallest thrust force compared with the other configurations. The largest S/N ratios for this set, as displayed in Figure 9(b), confirm this observation.

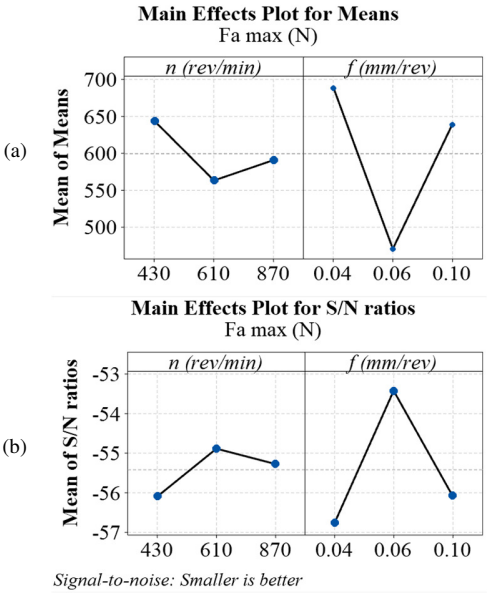

Fig. 9. Results of Taguchi experiment: (a) mean values and (b) S/N ratios.

TABLE IV. EXPERIMENTAL RESULTS OF F_{AMAX} (N)

Spindle speed n (rev/min)	Feed rate f (mm/rev)	Thrust force F_{amax} (N)			
		No.1	No.2	No.3	Average
430	0.04	696.2	707.7	693.1	699.1
430	0.06	514.2	521.7	531.8	522.6
430	0.10	712.3	708.5	709.1	710.0
610	0.04	657.6	665.4	654.2	659.1
610	0.06	441.1	435.5	440.3	439.0
610	0.10	595.1	589.4	588.5	591.0
870	0.04	718.5	707.7	698.1	708.0
870	0.06	439.3	447.1	460.7	449.0
870	0.10	612.6	610.9	621.8	615.0

D. Validation Test

Based on the results of the Taguchi experiment, a validation test was conducted using the selected parameter set. In the validation test, multi-hole drilling was performed with the optimized cutting parameters of n = 610 rev/min and f = 0.06 mm/rev, under internal lubrication with the proposed nanofluid. Additionally, to assess the positive effect of the nanofluid on lubrication, an experiment was conducted using the same cutting parameters but with a conventional emulsion fluid. The experimental results revealed that a new drill bit, internally cooled using the proposed nanofluid, could successfully complete up to 28 holes without breaking. In contrast, the new drill bit using the conventional emulsion fluid managed to complete only 16 holes before failure.

Figure 10 presents the mean and distribution of the thrust force obtained for each hole during the drilling process using the two types of lubricant. The mean thrust force using the nanofluid was approximately 2.0 times lower than that using the conventional emulsion, even when the drill bit was still totally new. Overall, the mean thrust force slightly increased as more holes were drilled compared to the first hole. However, the rate of increase was lower when using nano-fluid. The maximum thrust force induced by the nanofluid, observed at the 26th hole, was approximately 505.5 N. This value remained within the normal operating range, in contrast to the approximately 1550 N thrust force observed when the drill bit broke, as shown in Figure 3(b). Additionally, the distribution range of the thrust forces when drilling with the nanofluid was significantly smaller than that when drilling with the conventional emulsion fluid. The increasing trend in the thrust force can be attributed to the continuous wear and degradation of the drill bit during the cutting process. However, due to the enhanced lubricating efficiency of the nanofluid, the wear and breakage of the drill bit were significantly reduced. Moreover, compared to a previous study involving stationary drills [25], the thrust force generated using the rotary drill bit was significantly lower under nearly identical cutting conditions. Furthermore, the number of holes successfully completed was substantially higher with the rotary drilling method.

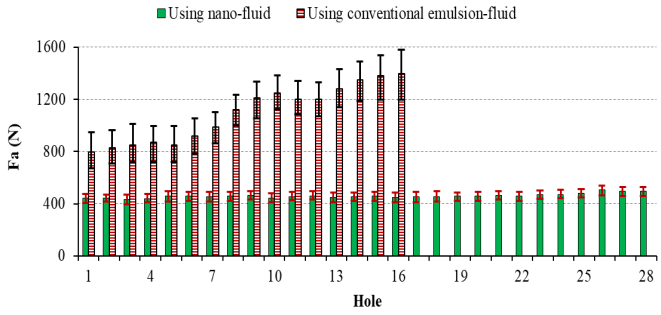

Fig. 10. Mean and distribution of thrust force for each drilled hole using the two lubricants under a spindle speed of 610 rev/min and a feed rate of 0.06 mm/rev.

The increase in thrust force observed when drilling subsequent holes, as portrayed in Figure 10, can be directly attributed to the cutting tool wear. Figure 11(a) shows the drill bits after completing 15 holes using the emulsion fluid, wherein one cutting edge exhibits significant wear, whereas the other is fractured. Additionally, the flank face shows extensive abrasion marks. Flank face wear arises from continuous friction between the tool and workpiece, resulting in elevated cutting forces and reduced tool life [7]. Cutting edge wear is characterized by gradual degradation that compromises cutting precision and likely contributes to the rise in thrust force over time [28]. In contrast, cutting edge breakage refers to severe fractures in the cutting zone, potentially caused by excessive cutting force or chip clogging, which drastically diminish tool performance [29]. These combined wear mechanisms led to increased cutting forces and a decline in cutting efficiency. Ultimately, chip deformation, breakage, and clogging accelerated drill-bit failure, as evidenced by its inability to complete even one hole in the pilot experiment.

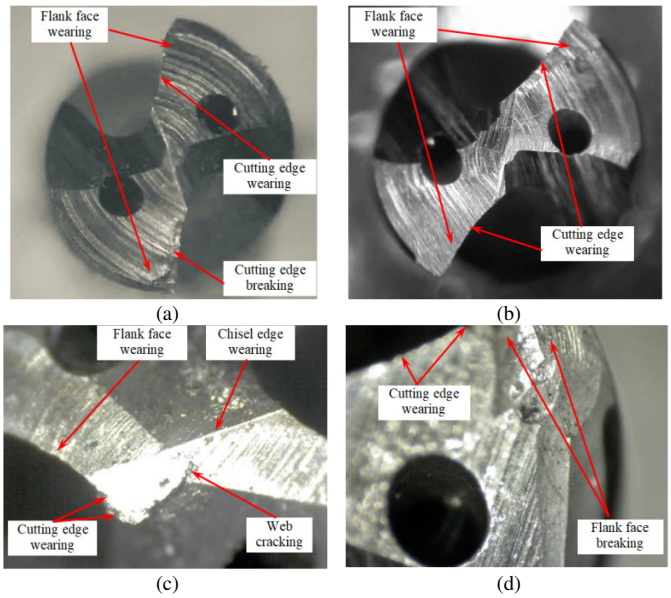

Fig. 11. Images of drill bits after drilling: (a)15 holes with conventional emulsion fluid, (b) 15 holes with nanofluid, and (c, d) 28 holes with nanofluid under a spindle speed of 610 rev/min and a feed rate of 0.06 mm/rev.

Figure 11(b) shows the drill bit after completing 15 holes using the proposed nanofluid lubrication. The cutting edges and flank faces exhibited only slight wear. This can be attributed to improved chip evacuation resulting from reduced friction, lower deformability, smaller chip width, and smoother surfaces, as observed in the pilot experiment. Additionally, this finding aligns with the slight increase in thrust force obtained after each hole was drilled.

Figures 11(c) and 11(d) present the images of the drill bit after drilling 28 holes using the graphene nanofluid. The chisel edge exhibited slight wear, whereas the flank faces showed significant wear and breakage. At the center of the flank face, small pitting and scratches appeared due to friction between the tool and the workpiece. Wear at the cutting edges was relatively complex, with minor wear observed near the tool center, whereas larger wear and breakage occurred near the drill's cylindrical surface. These fractures reduce the cutting efficiency of the drill bit, leading to an increase in the material removal force. This can be considered the primary cause of the increase in the thrust force observed when drilling later holes.

These findings are particularly significant in light of the transition from the stationary drilling setup employed in previous studies [17, 25] to the rotary drill configuration adopted in this work. In rotary drilling, the drill bit rotates at high speeds while engaging with the workpiece, which intensifies frictional heating, chip adhesion, and tool wear mechanisms. This substantially increases the demand for lubrication systems. Despite these harsher conditions, the graphene-based nanofluid, originally developed for low-viscosity delivery through internal channels, continued to perform effectively, validating its robustness and adaptability to real-world machining environments. Moreover, unlike most nanofluid systems that require deionized water to maintain stability and dispersion, the proposed formulation employs ordinary tap water, enabled by the emulsion-based carrier. This feature significantly lowers the cost and complexity of implementation, making it highly practical for shop-floor applications. Together, these contributions represent a meaningful advancement toward sustainable and scalable lubrication strategies for deep drilling of hard-to-cut materials.

IV. CONCLUSIONS

In this study, the application of a graphene-based nanofluid for deep-hole drilling of SUS 304 stainless steel using a rotary twist drill with internal coolant channels was investigated. Four experimental stages were conducted to evaluate the performance under low-pressure, low-flow rate conditions.

The pilot testing confirmed that the graphene-based nanofluid enabled successful drilling across all cutting parameters, including high feed rates, where the conventional emulsion failed.

The thrust force and chip morphology analyses revealed that the graphene-based nanofluid produced narrower and smoother chips with reduced deformation and adhesion, resulting in more efficient evacuation and lower cutting forces. The statistical tests confirmed a significant reduction in the thrust force and improved process stability.

A Taguchi design was employed to identify the optimal cutting parameters (610 rev/min spindle speed and 0.06 mm/rev feed rate), which were validated in multi-hole drilling trials. Under these conditions, the proposed nanofluid extended the tool life, completing 28 holes without failure, compared to only 16 holes opened with the conventional emulsion.

Although the graphene-based nanofluid formulation was previously validated under stationary drilling, this study demonstrates its effectiveness in rotary drilling, where the thermal and mechanical demands are substantially higher. The continued performance under these harsher conditions confirms the robustness and industrial viability of the approach. Moreover, the use of tap water, enabled by the emulsion-based carrier, eliminates the need for deionized water or high-pressure systems, offering a low-cost, scalable solution for machining hard-to-cut materials. These findings represent an advancement toward sustainable lubrication strategies for deep-hole drilling.

ACKNOWLEDGMENT

The authors gratefully acknowledge the support provided by the Thai Nguyen University of Technology, Vietnam.

REFERENCES

[1] B. Suresh Kumar, N. Baskar, and K. Rajaguru, "Drilling operation: A review," *Materials Today: Proceedings*, vol. 21, pp. 926–933, Jan. 2020, https://doi.org/10.1016/j.matpr.2019.08.160.

[2] R. Heinemann, S. Hinduja, G. Barrow, and G. Petuelli, "The Performance of Small Diameter Twist Drills in Deep-Hole Drilling," *Journal of Manufacturing Science and Engineering*, vol. 128, no. 4, pp. 884–892, Apr. 2006, https://doi.org/10.1115/1.2335859.

[3] S. A. Khan, A. Nazir, M. P. Mughal, M. Q. Saleem, A. Hussain, and Z. Ghulam, "Deep hole drilling of AISI 1045 via high-speed steel twist drills: evaluation of tool wear and hole quality," *The International Journal of Advanced Manufacturing Technology*, vol. 93, no. 1, pp. 1115–1125, Oct. 2017, https://doi.org/10.1007/s00170-017-0587-4.

[4] C. Han, D. Zhang, M. Luo, and B. Wu, "Chip evacuation force modelling for deep hole drilling with twist drills," *The International Journal of Advanced Manufacturing Technology*, vol. 98, no. 9, pp. 3091–3103, Oct. 2018, https://doi.org/10.1007/s00170-018-2488-6.

[5] N. A. Bassiouny, M. Al-Makky, and H. Youssef, "Parameters affecting the quality of friction drilled holes and formed thread in austenitic stainless steel AISI 304," *The International Journal of Advanced Manufacturing Technology*, vol. 125, no. 3, pp. 1493–1509, Mar. 2023, https://doi.org/10.1007/s00170-022-10788-x.

[6] A. Baumann, E. Oezkaya, D. Schnabel, D. Biermann, and P. Eberhard, "Cutting-fluid flow with chip evacuation during deep-hole drilling with twist drills," *European Journal of Mechanics - B/Fluids*, vol. 89, pp. 473–484, Sep. 2021, https://doi.org/10.1016/j.euromechflu.2021.07.003.

[7] E. Oezkaya, S. Michel, and D. Biermann, "Experimental and computational analysis of the coolant distribution considering the viscosity of the cutting fluid during machining with helical deep hole drills," *Advances in Manufacturing*, vol. 10, no. 2, pp. 235–249, Jun. 2022, https://doi.org/10.1007/s40436-021-00383-w.

[8] A. Eltaggaz and I. Deiab, "Comparison of between direct and peck drilling for large aspect ratio in Ti-6Al-4V alloy," *The International Journal of Advanced Manufacturing Technology*, vol. 102, no. 9, pp. 2797–2805, Jun. 2019, https://doi.org/10.1007/s00170-019-03314-z.

[9] Xu K., Yang Y., Feng W., Wan M., and Zhang W., "Internal cooling techniques in cutting process: A review," *Journal of Advanced Manufacturing Science and Technology*, vol. 4, no. 4, Apr. 2024, Art. no. 2024013, https://doi.org/10.51393/j.jamst.2024013.

[10] R. Arif, G. Fromentin, F. Rossi, and B. Marcon, "Investigations on drilling performance of high resistant austenitic stainless steel," *Journal*

of Manufacturing Processes, vol. 56, pp. 856–866, Aug. 2020, https://doi.org/10.1016/j.jmapro.2020.05.038.

[11] S. A. Khan, S. Shamail, S. Anwar, A. Hussain, S. Ahmad, and M. Saleh, "Wear performance of surface treated drills in high speed drilling of AISI 304 stainless steel," *Journal of Manufacturing Processes*, vol. 58, pp. 223–235, Oct. 2020, https://doi.org/10.1016/j.jmapro.2020.08.022.

[12] T. Aized and M. Amjad, "Quality improvement of deep-hole drilling process of AISI D2," *The International Journal of Advanced Manufacturing Technology*, vol. 69, no. 9, pp. 2493–2503, Dec. 2013, https://doi.org/10.1007/s00170-013-5178-4.

[13] Z. Zhang, L. Wu, S. Jia, and T. Peng, "Multi-objective parameter optimization to support energy-efficient peck deep-hole drilling processes with twist drills," *The International Journal of Advanced Manufacturing Technology*, vol. 106, no. 11, pp. 4913–4932, Feb. 2020, https://doi.org/10.1007/s00170-020-04967-x.

[14] D. A. Stephenson, E. Hughey, and A. A. Hasham, "Air flow and chip removal in minimum quantity lubrication drilling," *Procedia Manufacturing*, vol. 34, pp. 335–342, Jan. 2019, https://doi.org/10.1016/j.promfg.2019.06.171.

[15] A. Gandarias, L. N. Lopez de Lacalle, X. Aizpitarte, and A. Lamikiz, "Study of the performance of the turning and drilling of austenitic stainless steels using two coolant techniques," *International Journal of Machining and Machinability of Materials*, vol. 3, no. 1–2, pp. 1–17, Jan. 2008, https://doi.org/10.1504/IJMMM.2008.017621.

[16] M. L. Polli and M. J. Cardoso, "Effects of process parameters and drill point geometry in deep drilling of SAE 4144M under MQL," *Journal of the Brazilian Society of Mechanical Sciences and Engineering*, vol. 40, no. 3, Feb. 2018, Art. no. 137, https://doi.org/10.1007/s40430-018-1062-3.

[17] T.-D. Hoang *et al.*, "Ultrasonic assisted nano-fluid MQL in deep drilling of hard-to-cut materials," *Materials and Manufacturing Processes*, vol. 37, no. 6, pp. 712–721, Apr. 2022, https://doi.org/10.1080/10426914.2021.1981936.

[18] N.-H. Chu and V. Q. Vu, "Torque evaluation in ultrasonic-assisted deep hole drilling of AISI-304 stainless steel," *Machining Science and Technology*, vol. 29, no. 4, pp. 623–652, Jul. 2025, https://doi.org/10.1080/10910344.2025.2513032.

[19] J. Rajaguru and N. Arunachalam, "Effect of ultrasonic vibration on the performance of deep hole drilling process," *Procedia Manufacturing*, vol. 53, pp. 260–267, Jan. 2021, https://doi.org/10.1016/j.promfg.2021.06.029.

[20] E. Oezkaya, I. Iovkov, and D. Biermann, "Fluid structure interaction (FSI) modelling of deep hole twist drilling with internal cutting fluid supply," *CIRP Annals*, vol. 68, no. 1, pp. 81–84, Jan. 2019, https://doi.org/10.1016/j.cirp.2019.03.003.

[21] S. Hu *et al.*, "Nanoparticle-enhanced coolants in machining: mechanism, application, and prospects," *Frontiers of Mechanical Engineering*, vol. 18, no. 4, Jan. 2024, Art. no. 53, https://doi.org/10.1007/s11465-023-0769-8.

[22] A. Bhowmik *et al.*, "A comprehensive review on the viability of minimum quantity lubrication technology for machining difficult-to-cut alloys," *AIP Advances*, vol. 15, no. 3, Mar. 2025, Art. no. 030702, https://doi.org/10.1063/5.0256932.

[23] N. M. M. Reddy and P. K. Chaganti, "Investigating Optimum SiO2 Nanolubrication During Turning of AISI 420 SS," *Engineering, Technology & Applied Science Research*, vol. 9, no. 1, pp. 3822–3825, Feb. 2019, https://doi.org/10.48084/etasr.2537.

[24] A. G. N. Sofiah, M. Samykano, A. K. Pandey, K. Kadirgama, K. Sharma, and R. Saidur, "Immense impact from small particles: Review on stability and thermophysical properties of nanofluids," *Sustainable Energy Technologies and Assessments*, vol. 48, Dec. 2021, Art. no. 101635, https://doi.org/10.1016/j.seta.2021.101635.

[25] T.-D. Hoang, T.-H. Mai, and V.-D. Nguyen, "Enhancement of Deep Drilling for Stainless Steels by Nano-Lubricant through Twist Drill Bits," *Lubricants*, vol. 10, no. 8, Aug. 2022, Art. no. 173, https://doi.org/10.3390/lubricants10080173.

[26] A. Pal, S. S. Chatha, and H. S. Sidhu, "Experimental investigation on the performance of MQL drilling of AISI 321 stainless steel using nano-graphene enhanced vegetable-oil-based cutting fluid," *Tribology International*, vol. 151, Nov. 2020, Art. no. 106508, https://doi.org/10.1016/j.triboint.2020.106508.

[27] Z. Liao, D. Xu, D. Axinte, R. M'Saoubi, J. Thelin, and A. Wretland, "Novel cutting inserts with multi-channel irrigation at the chip-tool interface: Modelling, design and experiments," *CIRP Annals*, vol. 69, no. 1, pp. 65–68, Jan. 2020, https://doi.org/10.1016/j.cirp.2020.04.028.

[28] A. Faraz, D. Biermann, and K. Weinert, "Cutting edge rounding: An innovative tool wear criterion in drilling CFRP composite laminates," *International Journal of Machine Tools and Manufacture*, vol. 49, no. 15, pp. 1185–1196, Dec. 2009, https://doi.org/10.1016/j.ijmachtools.2009.08.002.

[29] S. R. Fernandez-Vidal, S. Fernandez-Vidal, M. Batista, and J. Salguero, "Tool Wear Mechanism in Cutting of Stack CFRP/UNS A97075," *Materials*, vol. 11, no. 8, Aug. 2018, Art. no. 1276, https://doi.org/10.3390/ma11081276.